

Chapter 13

The Utility of Stable and Radioisotopes in Fish Tissues as Biogeochemical Tracers of Marine Oil Spill Food Web Effects



William F. Patterson III, Jeffery P. Chanton, David J. Hollander, Ethan A. Goddard, Beverly K. Barnett, and Joseph H. Tarnecki

Abstract Direct exposure to petroleum compounds was widely reported for a variety of taxa following the DWH. Evidence of exposure ranged from oiling of skin, shells, or feathers, depending on the taxa, to observation of ingested oil in small translucent, invertebrates, to biomarkers of petroleum compounds within an organism's tissues, such as PAHs in the hepatopancreas of invertebrates or the liver of fishes, or metabolic products of PAH catabolism in the bile of various vertebrate taxa. Development of natural biogeochemical tracers to examine indirect effects, especially over long (months to years) time scales, can be much more problematic. In this chapter, we describe the utility of employing stable isotopes and radioisotopes to 1) examine whether food web effects can be inferred from shifts in stable isotope values measured in vertebrate taxa; 2) examine the assimilation and trophic transfer of petrocarbon in marine food webs; and, 3) serve as long-term biogeochemical tracers either of petrocarbon assimilation or trophic shifts that are indicative of food web effects of marine oil spills. Data and analyses are largely drawn from DWH-related studies but with broader implications to marine oil spills in general.

Keywords Petrocarbon · Reef fish · Stable isotopes · Radiocarbon

W. F. Patterson III (✉) · J. H. Tarnecki
University of Florida, Fisheries and Aquatic Sciences, Gainesville, FL, USA
e-mail: will.patterson@ufl.edu

J. P. Chanton
Florida State University, Department of Earth, Ocean and Atmospheric Science,
Tallahassee, FL, USA
e-mail: jchanton@fsu.edu

D. J. Hollander · E. A. Goddard
University of South Florida, College of Marine Science, St. Petersburg, FL, USA
e-mail: davidh@usf.edu; egoddard@usf.edu

B. K. Barnett
University of Florida, Fisheries and Aquatic Sciences, Gainesville, FL, USA
National Marine Fisheries Service, Southeast Fisheries Science Center, Panama City
Laboratory, Panama City, FL, USA
e-mail: beverly.barnett@noaa.gov

13.1 Introduction

Large-scale marine oil spills such as the *Deepwater Horizon* (DWH) oil spill have caused significant impacts to a broad diversity of taxa, from plankton to marine mammals, around the globe. Often, the impacts from these spills receiving the greatest attention are direct ones, such as mortality due to oiling of organisms or toxicological or physiological effects due to exposure to petroleum compounds, such as polycyclic aromatic hydrocarbons (PAHs). While the expression of direct impacts of spills is often acute, occurring in the minutes to days after a spill, other effects can be chronic and manifested for years thereafter.

Indirect effects of oil spills, such as altered food webs or the bioenergetic consequences of such changes, have received considerably less attention than direct effects (but see Gin et al. 2001; Peterson et al. 2003; McCann et al. 2017; Olin et al. 2018). This is likely due to the fact that direct effects are often easier to diagnose and track. One simply needs to find evidence of exposure to petroleum compounds, have an understanding of the toxicological or physiological consequences of that exposure, and then measure the response at the cellular, tissue, organ, or organismal level. Estimating indirect effects on organisms, populations, communities, or ecosystems is much less tractable for several reasons (Fodrie et al. 2014; Beyer et al. 2016). First, one must have baseline data to understand pre-spill conditions and natural variability (process error) in the parameters of interest. Then, one must have a way to measure and track indirect effects over time that is independent of the markers utilized to estimate direct exposure to petroleum compounds. Ideally, these markers would not be ephemeral but instead would have some level of permanence such that chronic impacts of indirect effects could be examined years to decades after a spill.

Evidence of direct exposure to petroleum compounds can range from oiling of skin, shells, or feathers, depending on the taxa, to observation of ingested oil in small translucent, invertebrates, to biomarkers of petroleum compounds within an organism's tissues, such as PAHs in the hepatopancreas of invertebrates or the liver of fishes, or metabolic products of PAH catabolism in the bile of various vertebrate taxa. Development of natural biogeochemical tracers to examine indirect effects, especially over long (months to years) time scales, can be much more problematic. However, natural biogeochemical tracers described in earlier chapters of this book, in the form of stable isotope ratios measured in tissues of various taxa, may be ideal for inferring changes in food web structure and prey resource availability following a marine oil spill. Furthermore, depleted $\Delta^{14}\text{C}$ values in tissues may indicate petrocarbon assimilated into and transferred through the marine food web, thus providing a natural tracer of the footprint of an oil spill's effects (e.g., Wilson et al. 2016). Therefore, the objectives of this chapter are to describe the utility of employing stable isotopes and radioisotopes to (1) examine whether food web effects can be inferred from shifts in stable isotope values measured in reef fishes, (2) examine the assimilation and trophic transfer of petrocarbon in marine food webs, and (3) serve as long-term biogeochemical tracers either of petrocarbon assimilation or trophic

shifts that are indicative of food web effects of marine oil spills. Data and analyses are drawn from DWH-related studies but with broader implications to marine oil spills in general.

13.2 Stable Isotopes Utilized to Infer Food Web Effects

Stable isotopes are widely utilized in marine ecology to infer sources of organic carbon, estimate trophic position, and examine food web connectivity (Fry 2006). The most widely utilized stable isotope ratios in ecology are those of C and N, expressed as the delta values $\delta^{13}\text{C}$ and $\delta^{15}\text{N}$. In each case, a stable isotope delta value is computed as the ratio of a lighter to heavier stable isotope of a given element in a sample relative to a standard with the following equation:

$$\delta X = \left[\left(R_{\text{sample}} / R_{\text{standard}} \right) - 1 \right] * 10^3, \quad (13.1)$$

where $X = {}^{13}\text{C}$ or ${}^{15}\text{N}$, $R = {}^{13}\text{C}/{}^{12}\text{C}$ or ${}^{15}\text{N}/{}^{14}\text{N}$, standards are N in air ($\delta^{15}\text{N}_{\text{Air}}$) for $\delta^{15}\text{N}$ and Pee Dee Belemnite ($\delta^{13}\text{C}_{\text{V-PDB}}$) for $\delta^{13}\text{C}$, and units of δX are ‰ or per mille. For a given element, its stable isotopes only differ by the number of neutrons. Therefore, different stable isotopes for that element have different atomic masses but have slightly slower chemical reaction kinetics. In turn, this results in the products of reactions, including metabolic reactions in organisms, having different (heavier) isotopic ratios.

Physiological differences in primary producers drive differences in basal $\delta^{13}\text{C}$ values, which then can be utilized to distinguish different sources of organic C and trophic pathways in marine ecosystems. However, on the northern Gulf of Mexico (nGoM) shelf, the predominant primary producers are benthic microalgae (BMA, $\sim -19\text{‰}$) and phytoplankton ($\sim -21\text{‰}$), which differ very little in $\delta^{13}\text{C}$ (Moncrieff and Sullivan 2001; Radabaugh et al. 2013; Tarnecki and Patterson 2015). Furthermore, there is no significant difference in the $\delta^{15}\text{N}$ values between nGoM phytoplankton and BMA (Radabaugh et al. 2013; Tarnecki and Patterson 2015), with mean basal $\delta^{15}\text{N}$ being 5.82‰ among baseline BMA and phytoplankton samples collected on the north central GoM shelf prior to the DWH (Tarnecki and Patterson 2015).

Having accurate estimates of basal $\delta^{13}\text{C}$ and $\delta^{15}\text{N}$ values is critical to examining food web dynamics with stable isotope ratios. As organic matter is consumed and assimilated by organisms at progressively higher trophic positions, $\delta^{13}\text{C}$ and $\delta^{15}\text{N}$ values increase due to the metabolic process of trophic fractionation (Fry 2006). Given that reaction kinetics of the lighter isotope, ${}^{12}\text{C}$ in the case of C and ${}^{14}\text{N}$ in the case of N, are slightly faster than with the heavier isotope (${}^{13}\text{C}$ or ${}^{15}\text{N}$), the metabolic processes of digestion and assimilation result in the isotopic ratios becoming enriched in the heavier isotopes of C and N, thus the $\delta^{13}\text{C}$ and $\delta^{15}\text{N}$ values increasing at progressively higher trophic positions. If one has an estimate of the basal values, particularly for $\delta^{15}\text{N}$, and an estimate of the trophic discrimination factor (TDF), or

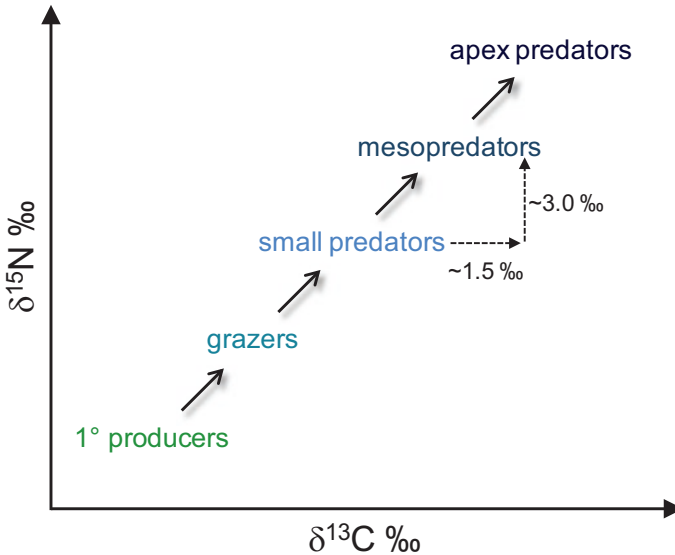


Fig. 13.1 Conceptual model of trophic fractionation of muscle tissue that occurs as organic matter is consumed and assimilated by organisms at progressively higher trophic levels. Trophic discrimination factor estimates are 3.0‰ for $\delta^{15}\text{N}$ and 1.5‰ for $\delta^{13}\text{C}$ (see text for details)

the per mille increase in $\delta^{15}\text{N}$ per trophic position, then one can estimate the trophic position of a given individual from its measured $\delta^{15}\text{N}$ value.

Trophic discrimination factors differ by element as well as by the tissue being examined. In marine ecology, muscle tissue is often analyzed due its relatively long (months) turnover time, which implies a trophic signature integrated over that time period. In the case of bony fish muscle, the TDF for $\delta^{13}\text{C}$ ($\Delta^{13}\text{C}$) estimated across a range of experiments and studies is approximately 1.5‰ (Sweeting et al. 2007). The TDF for $\delta^{15}\text{N}$ ($\Delta^{15}\text{N}$) is approximately 3.0‰, which is the mean measured for fishes feeding on high-protein diets (McCutchan et al. 2003; Vanderklift and Ponsard 2003; Rooker et al. 2006). Therefore, at progressively higher trophic levels, one would expect an increase in $\delta^{13}\text{C}$ of approximately 1.5‰ and an increase in $\delta^{15}\text{N}$ of approximately 3.0‰, resulting in a positive slope in the relationship between $\delta^{15}\text{N}$ and $\delta^{13}\text{C}$ when a bi-plot of those parameters is constructed across different trophic levels within a marine food web (Fig. 13.1).

13.2.1 Temporal Variability in Reef Fish Muscle Stable Isotopes

The general relationship between $\delta^{15}\text{N}$ and $\delta^{13}\text{C}$ enables the usage of stable isotopes to examine food web structure, as well as to examine shifts in that structure resulting from disturbance. For example, stable isotopes have been utilized to examine

marine trophic shifts due to eutrophic phytoplankton blooms and habitat degradation (Chasar et al. 2005), effects of chronic trawling and overfishing (Jennings et al. 2002), and large-scale aquaculture operations (Holmer et al. 2007). Therefore, as long as pre-disturbance stable isotope data are available, trophic shifts or food web effects can be inferred by examining stable isotopes in post-disturbance samples.

In the case of the DWH, Tarnecki and Patterson (2015) reported significant post-DWH diet shifts in red snapper, *Lutjanus campechanus*, a reef fish that is a ubiquitous member of natural and artificial reef communities in the nGoM. Red snapper are extreme generalists, with their diet ranging from swarming zooplankton to fish (McCawley et al. 2003; Tarnecki and Patterson 2015). Therefore, they are an ideal candidate to examine post-DWH diet shifts. Following the spill, plankton disappeared from red snapper diet, and benthic and demersal fishes constituted a much larger percentage of observed prey. These diet shifts were also apparent in white muscle stable isotope values, as $\delta^{15}\text{N}$ increased and $\delta^{34}\text{S}$ declined in post-DWH samples, although stable isotope shifts lagged behind diet shifts due to the turnover time in their white muscle tissue being approximately 6 months (Nelson et al. 2011). While $\delta^{15}\text{N}$ is indicative of trophic position, $\delta^{34}\text{S}$ serves as an effective biomarker of pelagic versus benthic production (Fry 2006). For example, nGoM phytoplankton $\delta^{34}\text{S}$ is approximately 20‰, while BMA has a value of approximately 10‰ (Moncrieff and Sullivan 2001; Tarnecki and Patterson 2015). These distinctive signatures are due to sulfate, SO_4^{2-} , being the predominant source of S in the water column, while it is reduced to sulfide (S^{2-}) by bacteria in the benthos (Fry and Chumchal 2011). Given only minimal trophic fractionation ($\sim 0.5\text{‰}$ per trophic level) in $\delta^{34}\text{S}$, it effectively distinguishes pelagic versus benthic production sources (Fry 2006).

The red snapper white muscle stable isotope data reported by Tarnecki and Patterson (2015) were updated through April 2015 to demonstrate trends in $\delta^{15}\text{N}$ and $\delta^{13}\text{C}$ from the year prior to the DWH through 5 years post-spill. Adult red snapper samples were collected with hook-and-line sampling at natural and artificial reefs across the north central GoM shelf between 15 and 80 m water depths in a $\sim 7500\text{ km}^2$ region bracketed by $86^\circ 14' \text{ W}$ and $88^\circ 59' \text{ W}$ longitude. White muscle tissue was freeze-dried and analyzed for $\delta^{15}\text{N}$ and $\delta^{13}\text{C}$ with either a Europa Scientific GSL/Geo 20–20 stable isotope ratio-mass spectrometer (SIR-MS) or with a Thermo Delta+XL SIR-MS. Both SIR-MS instruments were coupled with elemental analyzers to estimate %C and %N, hence C:N, in each sample. Because lipids are depleted in ^{13}C relative to muscle protein, and C:N ratio serves as an effective proxy of lipid content in fish muscle samples, all $\delta^{13}\text{C}$ data reported below were first corrected for lipid content with the equation reported by Post et al. (2007):

$$\text{CF} = -3.32 + (0.99 * \text{C} : \text{N}), \quad (13.2)$$

where CF is the correction factor applied to $\delta^{13}\text{C}$ to account for percent lipid in dried muscle samples and C:N serves as a proxy for percent lipid.

There were 400 red snapper muscle tissue samples analyzed across 6 years (Table 13.1, Fig. 13.2a), with two trends apparent in the data. First, $\delta^{15}\text{N}$ increased approximately 0.7‰, or one-quarter of a trophic position, between the pre-spill period and year-3 post-DWH (Fig. 13.2a) and then returned to near pre-DWH levels.

Table 13.1 Sample sizes for northern Gulf of Mexico reef fish muscle tissue samples ($n = 846$) analyzed for $\delta^{15}\text{N}$ and $\delta^{13}\text{C}$ in the year prior to and the 5 years following the *Deepwater Horizon* oil spill

Species	Pre-DWH	Year-1	Year-2	Year-3	Year-4	Year-5	Total
gray triggerfish	8	28	40	18	15	6	115
red porgy	10	42	24	4	22	5	107
red snapper	52	133	71	43	76	25	400
tomtate	19	20	29	17	10	5	100
vermilion snapper	12	35	27	11	28	11	124

Sample locations were between $86^{\circ} 14'$ and $88^{\circ} 59'$ west longitude at depths of 15–80 m across the shelf

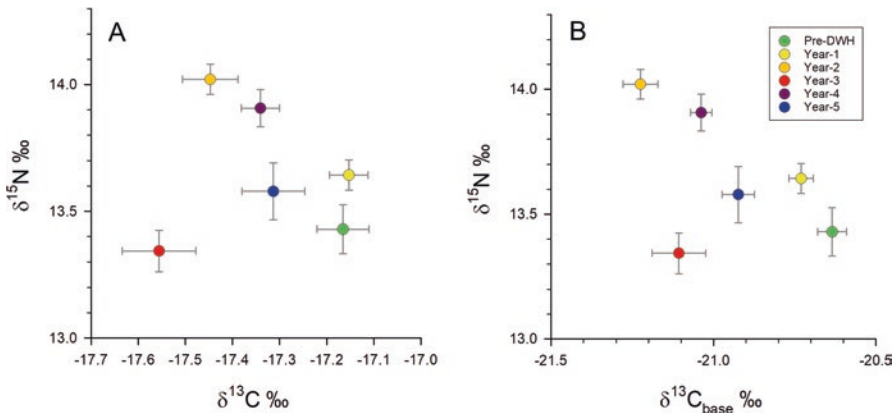


Fig. 13.2 Bi-plots of northern Gulf of Mexico red snapper muscle (a) $\delta^{15}\text{N}$ versus $\delta^{13}\text{C}$ for fish sampled the year prior to and during the 5 years following the *Deepwater Horizon* oil spill and (b) $\delta^{15}\text{N}$ versus $\delta^{13}\text{C}$ estimated at the base of the food web ($\delta^{13}\text{C}_{\text{base}}$) to account for shifts in trophic position inferred from shifts in $\delta^{15}\text{N}$ observed following the spill (see text for details). Error bars are \pm standard error of the mean

Secondly, instead of $\delta^{13}\text{C}$ increasing with $\delta^{15}\text{N}$, which would follow the general pattern indicated in Fig. 13.1, $\delta^{13}\text{C}$ actually decreased (Fig. 13.2a), which indicates a lighter source of organic C in the system. Tarnecki and Patterson (2015) inferred this trend in $\delta^{13}\text{C}$ most likely resulted from the trophic transfer and assimilation of petrocarbon in the food web. However, understanding $\delta^{13}\text{C}$ dynamics is complicated due to trophic fractionation that occurs in $\delta^{13}\text{C}$. Therefore, trophic position was controlled for in $\delta^{13}\text{C}$ data, by estimating basal $\delta^{13}\text{C}$ ($\delta^{13}\text{C}_{\text{base}}$) for each muscle sample with the equation:

$$\delta^{13}\text{C}_{\text{base}} = \delta^{13}\text{C}_{\text{muscle}} - [(\text{trophic position} - 1) * \Delta_{\text{C}}], \tag{13.3}$$

where $\delta^{13}\text{C}_{\text{muscle}}$ is the measured $\delta^{13}\text{C}$ in a given muscle sample; trophic position is the trophic position of sample estimated from the measured $\delta^{15}\text{N}$ in the sample, a $\delta^{15}\text{N}_{\text{base}}$ value of 5.82‰ , and $\Delta^{15}\text{N} = 3.0\text{‰}$ per trophic level; and, $\Delta^{13}\text{C} = 1.5\text{‰}$ per trophic level.

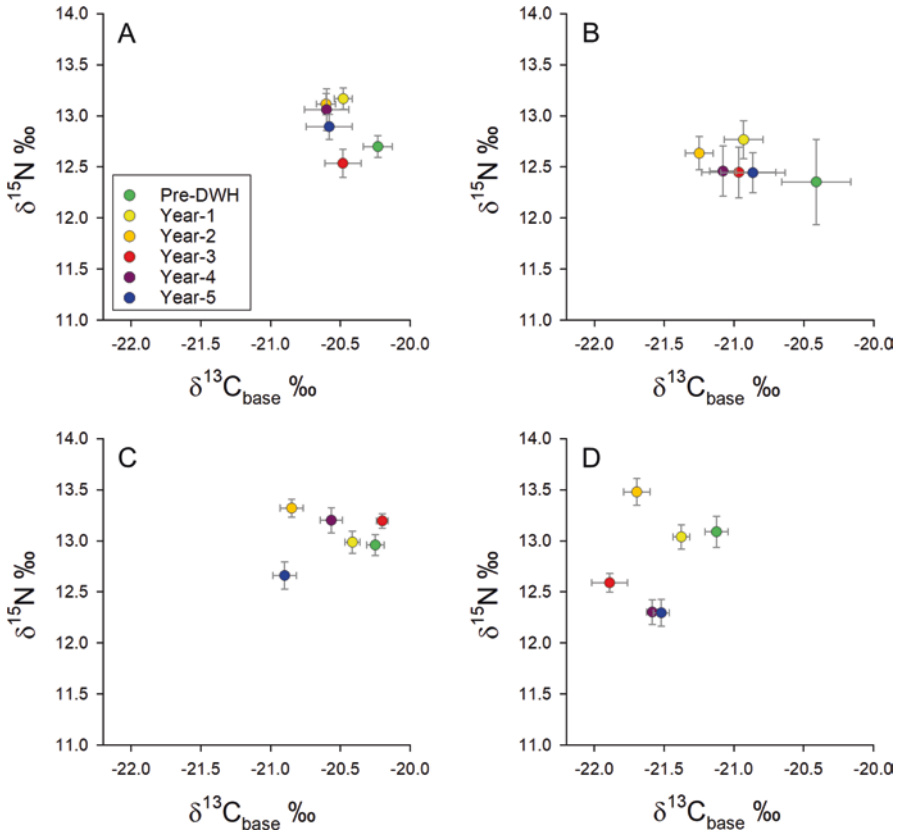


Fig. 13.3 Bi-plots of white muscle $\delta^{15}\text{N}$ versus $\delta^{13}\text{C}$ estimated at the base of the food web ($\delta^{13}\text{C}_{\text{base}}$) for northern Gulf of Mexico reef fishes: (a) gray triggerfish, (b) tomtate, (c) red porgy, and (d) vermilion snapper. Error bars are \pm standard error of the mean

The trend in lighter $\delta^{13}\text{C}_{\text{base}}$ over the first 3 years post-DWH is more pronounced than that observed for red snapper muscle $\delta^{13}\text{C}$ without correcting for trophic position (Fig. 13.2), thus more clearly indicating ^{13}C depletion following the DWH. Norberg (2015) reported similar patterns for tomtate, *Haemulon aurolineatum*, another ubiquitous reef fish in the nGoM which is predominantly an invertivore (Sedberry 1985; Norberg 2015). The narrower diet of tomtate meant nonsignificant shifts in muscle $\delta^{15}\text{N}$ were observed, but post-DWH declines in $\delta^{13}\text{C}$ were similar to those reported by Tarnecki and Patterson (2015).

Here, we report $\delta^{15}\text{N}$ and $\delta^{13}\text{C}_{\text{base}}$ for muscle tissue from additional reef fish species sampled in the same study region and during the same period as described above for red snapper (Fig. 13.3). These include tomtate; gray triggerfish, *Balistes capricus*, a demersal grazing invertivore with a diet comprised of benthic and encrusting invertebrates (Vose and Nelson 1994; Kurz 1995; Goldman et al. 2016); red porgy, *Pagrus pagrus*, a demersal reef omnivore (Manooch 1977; Goldman et al. 2016); and vermilion snapper, *Rhomboplites aurorubens*, a pelagic reef omnivore with a diet

nearly as broad as red snapper (Grimes 1979; Tarnecki et al. 2016). In all species, the shift in $\delta^{15}\text{N}$ was $\sim 0.5\text{‰}$ but was highest for vermilion snapper and lowest for tomte (Fig. 13.3). Like red snapper, muscle $\delta^{15}\text{N}$ had generally returned to near pre-DWH values by year-4 post-spill for these other reef fishes as well. However, vermilion snapper muscle $\delta^{15}\text{N}$ actually decreased below the pre-spill mean (Fig. 13.3d). It is unclear what drove that result; however, only 12 pre-spill vermilion snapper were sampled, and they came from a somewhat restricted area on the western side of the study region. Therefore, it is possible these fish were not representative of the entire region.

The shift in $\delta^{13}\text{C}_{\text{base}}$ observed among the additional reef fish species ranged from approximately 0.5 to 1.0‰ in the years following the DWH (Fig. 13.3), which brackets the pattern observed in red snapper samples (Fig. 13.2). However, the overall patterns are most easily observed when simply plotting the mean shifts in $\delta^{15}\text{N}$ versus $\delta^{13}\text{C}_{\text{base}}$ (Fig. 13.4). Among all species, the decline in mean $\delta^{13}\text{C}_{\text{base}}$ was approximately 0.6‰ by year-3. A transition back toward pre-spill values occurred thereafter, but $\delta^{13}\text{C}_{\text{base}}$ never fully returned to pre-DWH values during the 5 post-spill years.

The observed difference in $\delta^{13}\text{C}_{\text{base}}$ between pre-DWH and year-5 data, which is consistent across species, could be explained by a number of possible scenarios. Phytoplankton could have contributed a greater proportion of primary production relative to BMA in the post-spill time period, hence the lower $\delta^{13}\text{C}_{\text{base}}$ values. The actual difference ($\sim 0.3\text{‰}$) is so small that it could have been caused by any number of factors that potentially affect phytoplankton physiology (Leboulanger et al. 1995; Fry 2006). Lastly, if the decline in $\delta^{13}\text{C}_{\text{base}}$ observed between pre-DWH and year-3

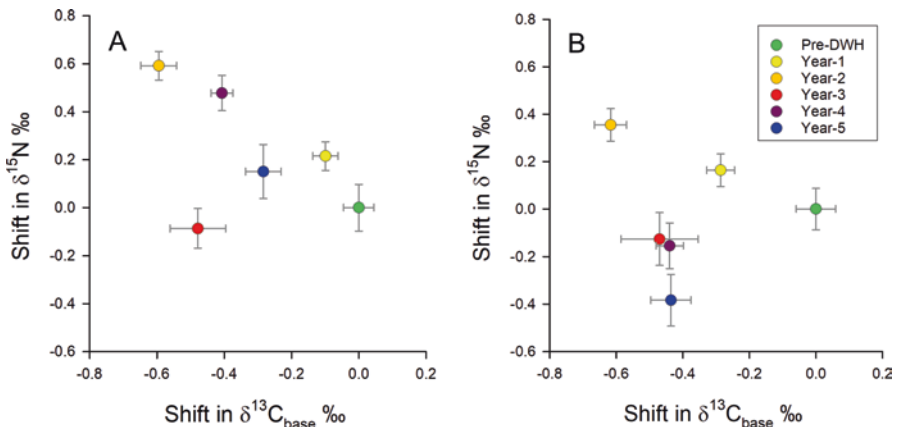


Fig. 13.4 Shifts in $\delta^{15}\text{N}$ versus those in $\delta^{13}\text{C}_{\text{base}}$ for (a) red snapper ($n = 400$) and (b) other reef fishes (gray triggerfish, $n = 115$; red pogy, $n = 107$; tomte, $n = 100$; and vermilion snapper, $n = 124$) observed in the years following the *Deepwater Horizon* oil spill relative to pre-spill mean values. Among the samples depicted in panel B, species-specific shifts were computed relative to species-specific mean pre-spill values; then mean annual shifts among all species across all samples were computed. Error bars are \pm standard error of the mean

samples was due to trophic transfer and assimilation of petrocarbon, then the persistence of organic carbon depleted in ^{13}C could be due to the retention and cycling of that signature in the nGoM food web. Evidence is presented below that supports the hypothesis that lower post-DWH $\delta^{13}\text{C}_{\text{base}}$ values in reef fish muscle tissue samples were in fact driven by the assimilation, trophic transfer, and retention of petrocarbon in the nGoM food web.

13.3 Petrocarbon Assimilation in the Gulf of Mexico Food Web

There are several lines of evidence demonstrating that petrocarbon was assimilated into lower trophic levels of the nGoM food web following the DWH. Micro- ($1\ \mu\text{m}$ – $0.2\ \text{mm}$) and meso- (0.2 – $20\ \text{mm}$) zooplankton sampled off Alabama (i.e., the western edge of the reef fish sample region described above) had depleted $\delta^{13}\text{C}$ signatures in summer 2010 that coincided with the arrival of surface oil slicks during the DWH event (Graham et al. 2010). The hydrocarbons released during the DWH had a $\delta^{13}\text{C}$ value of -27.2‰ for petroleum (Graham et al. 2010) and -57.4‰ for methane (Chanton et al. 2012), while mean $\delta^{13}\text{C}$ of nGoM particulate organic carbon (POM), which is a proxy for phytoplankton, is $\sim 20\text{‰}$ (Chanton et al. 2020). Therefore, Graham et al. (2010) inferred $\delta^{13}\text{C}$ values depleted in ^{13}C by $\sim 4\text{‰}$ in microzooplankton and $\sim 1\text{‰}$ in mesozooplankton relative to pre-spill values were indicative of bacterial assimilation of petroleum that was then transferred to two levels of consumers: first to microzooplankters, such as ciliates, and then to mesozooplankters, such as copepods. The authors discounted the potential for freshwater input from Mobile Bay to have affected plankton $\delta^{13}\text{C}$ values given the sampling occurred during a low-flow period and lower zooplankton $\delta^{13}\text{C}$ values closely corresponded with the arrival of surface oil slicks.

Results of subsequent ^{14}C analysis of nGoM plankton samples provide yet stronger evidence of petrocarbon assimilation and transfer in the nGoM food web. Radiocarbon (^{14}C) is a radioisotope and thus undergoes radioactive decay. It is typically reported as $\Delta^{14}\text{C}$, which is a measure of the relative difference in ^{14}C activity in a sample versus the absolute international standard (base year 1950) and corrected for age and fractionation via $\delta^{13}\text{C}$ (Stuiver and Pollach 1977). Its usage as a biomarker for petrocarbon is reviewed earlier in this book by Chanton et al. (2020). Briefly, modern surface organic C has a $\Delta^{14}\text{C}$ value of $\sim 40\text{‰}$, while petrocarbon, which is a fossil carbon that has been buried for millions of years such that all of its ^{14}C has been lost to radioactive decay, has a value of -1000‰ . Therefore, assimilated petrocarbon in nGoM biota following the DWH would cause a much greater depletion in $\Delta^{14}\text{C}$ than would be observed in $\delta^{13}\text{C}$ given the greater difference in $\Delta^{14}\text{C}$ versus $\delta^{13}\text{C}$ values of end-members (Wilson et al. 2016; Bosman et al. 2017).

Chanton et al. (2020) report utilizing $\Delta^{14}\text{C}$ as a biogeochemical tracer to examine petrocarbon in three different carbon pools in the nGoM: dissolved organic

carbon (DOC), sinking particulate organic carbon (POC_{sink}), and sedimentary organic matter (SOM). As they point out, these pools play important roles in carbon cycling in this ecosystem, as well as in nutrient cycling. However, our interest here is in yet another pool, which is assimilated carbon, specifically petrocarbon, in the biomass of living organisms (i.e., the food web). Toward that end, plankton sampled from the nGoM in 2010 and 2011 and analyzed by Chanton et al. (2012) for $\delta^{13}\text{C}$ with SIR-MS and for $\Delta^{14}\text{C}$ with accelerator mass spectrometry (AMS) produced a significant linear relationship between $\delta^{13}\text{C}$ and $\Delta^{14}\text{C}$ values. The authors concluded these results indicated an admixture existed in zooplankton biomass between ^{13}C - and ^{14}C -depleted material and modern organic carbon fixed by phytoplankton. Furthermore, they concluded their data supported the inference of Graham et al. (2010) that petrocarbon consumed and assimilated by bacteria had been transferred into the metazoan food web via mesozooplankton grazing on microzooplankters but suggested methane instead of petroleum might be the source of petrocarbon. Later, based on SIR-MS and AMS analysis of POC samples taken off the shelf to a depth of 1200 m, Cherrier et al. (2013) clearly demonstrated that methane was in fact the most likely source of petrocarbon found in nGoM plankton following the DWH. The questions that follow are whether DWH-derived petrocarbon was effectively transferred to higher trophic levels and whether more permanent biomarkers than muscle protein may have recorded this signal.

13.3.1 Radiocarbon Analysis of Reef Fish Muscle Tissue

The archive of freeze-dried reef fish muscle tissue samples described above provided an opportunity to examine whether petrocarbon assimilated into the nGoM microbial food web, and then transferred via grazing zooplankton into the metazoan food web, made it to the level of mesopredator reef fishes. To test this, red snapper muscle tissue samples ($n = 15$) were analyzed for $\delta^{13}\text{C}$ with SIR-MS and for $\Delta^{14}\text{C}$ with AMS at the Center for Applied Isotope Studies (CAIS) University of Georgia or the National Ocean Sciences Accelerator Mass Spectrometry (NOSAMS) at Woods Hole Oceanographic Institution. Samples were randomly selected from among the 400 dried tissues and transferred to CAIS or NOSAMS. They were first subjected to H_3PO_4 in closed, evacuated glass vessels. The produced CO_2 was then stripped and cryogenically purified from H_2O vapor and N_2 . A portion of the purified CO_2 was analyzed for $\delta^{13}\text{C}$ with SIR-MS, and the remainder was transferred to a reaction tube and reduced to pure C (graphite) in the presence of H_2 gas and Fe as a catalyst. The graphite was then pressed into target cartridges and analyzed for ^{14}C with AMS. Results are reported as $\Delta^{14}\text{C}$, which was corrected for natural isotopic fractionation via $\delta^{13}\text{C}$.

There is a significant linear relationship between $\Delta^{14}\text{C}$ and $\delta^{13}\text{C}_{\text{base}}$ among archived red snapper muscle samples, with the regression's coefficient of determination (R^2) being 0.48 (Fig. 13.5). This relationship confirms the decline in $\delta^{13}\text{C}_{\text{base}}$ observed in reef fish muscle tissue was due to petrocarbon being assimilated and

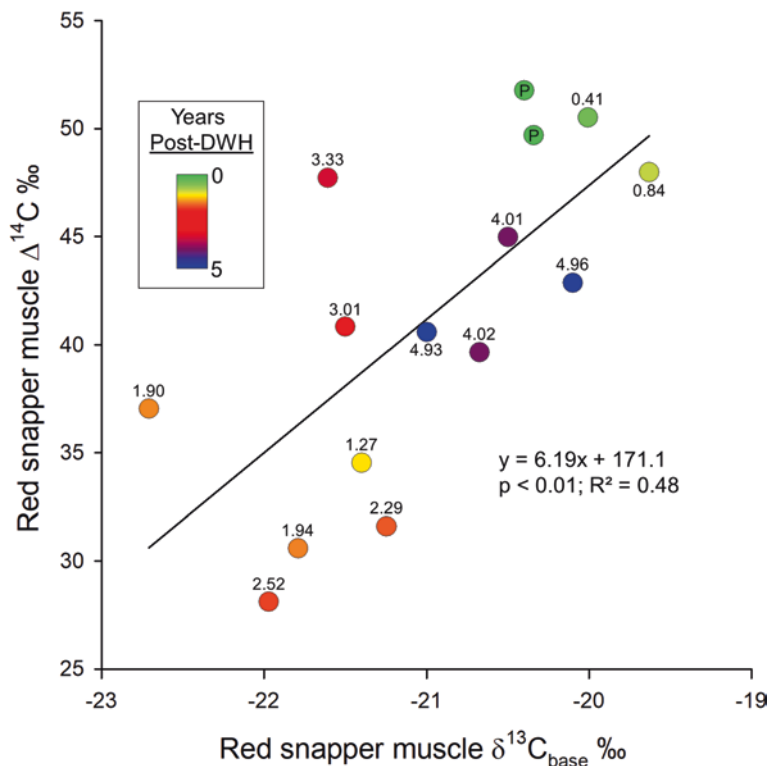


Fig. 13.5 Plot of red snapper muscle $\Delta^{14}\text{C}$ versus estimated $\delta^{13}\text{C}_{\text{base}}$ for fish sampled in the northern Gulf of Mexico the year before the *Deepwater Horizon* oil spill through 5 years post-spill. The legend indicates the timing of samples. Line indicates linear regression fit to the data. Numbers next to symbols on plot indicate years post-DWH; P = pre-spill samples

transferred up the metazoan food web. In fact, the relationship between red snapper muscle $\Delta^{14}\text{C}$ and $\delta^{13}\text{C}_{\text{base}}$ is actually slightly stronger than the one reported by Chanton et al. (2012) for nGoM zooplankton ($R^2 = 0.48$ versus 0.37). Furthermore, the slopes of the two relationships (6.2 for red snapper and 9.1 for plankton) are not significantly different, but that mostly owes to wide confidence intervals due to substantial unexplained variance in each model.

Red snapper muscle $\Delta^{14}\text{C}$ in the pre-spill period (2009 through early 2010) was higher (mean = 50.7‰) than mean $\Delta^{14}\text{C}$ reported by Chanton et al. (2012) for nGoM dissolved inorganic C (DIC, 41.0‰), which reflects complex dynamics in the system. For starters, shelf water DIC is affected by bomb ^{14}C that was input into the global ocean during nuclear weapon testing in the middle of the last century. The peak in $\Delta^{14}\text{C}$ occurred in ~1975, as inferred from coral records, with slight variation among ocean basins (Grottoli and Eakin 2007). There has been a linear decline since then (~2.6‰ per year in the nGoM; Barnett et al. 2018) due to mixing of bomb ^{14}C into the deep ocean. The fact that red snapper muscle tissue had higher $\Delta^{14}\text{C}$ than that of DIC reported by Chanton et al. (2012) is likely due to organic carbon

fixed with earlier DIC $\Delta^{14}\text{C}$ signatures being assimilated, transferred, and somewhat preserved in the standing stock of various taxa.

The trend in red snapper muscle $\Delta^{14}\text{C}$ suggests there was a lag of approximately 1 year between when zooplankton samples depleted in ^{14}C were first observed and when $\Delta^{14}\text{C}$ started declining in red snapper muscle tissue (Fig. 13.5). Furthermore, it was not until ~ 2.5 years post-spill that muscle $\Delta^{14}\text{C}$ values were at their lowest. Muscle $\Delta^{14}\text{C}$ increased during the last 2 years of the time series, but had not recovered to pre-DWH levels by 2014–2015, and no data currently exist to examine whether $\Delta^{14}\text{C}$ continued to increase after 2015. However, it may be that values of muscle $\Delta^{14}\text{C}$ observed in 2014–2015 did not increase further given $\Delta^{14}\text{C}$ was approximately 11‰ lower in 2014–2015 (year-5 post-DWH) than during 2009–2010, which is consistent with the predicted rate of decline in DIC $\Delta^{14}\text{C}$ over that time period (Barnett et al. 2018).

Red snapper muscle $\Delta^{14}\text{C}$ values have greater utility than simply certifying declines in reef fish muscle $\delta^{13}\text{C}_{\text{base}}$ resulted from petrocarbon or understanding the temporal progression of petrocarbon moving through the nGoM food web. Mixing models, such as those employed by Chanton et al. (2020), were applied to muscle $\Delta^{14}\text{C}$, as well as to $\delta^{13}\text{C}_{\text{base}}$, to estimate the percentage of carbon in red snapper muscle tissue derived from petrocarbon. The model employed to estimate percent petrocarbon from $\delta^{13}\text{C}_{\text{base}}$ for a given sample was:

$$\delta^{13}\text{C}_{\text{base}} = (f_1 * \delta^{13}\text{C}_{\text{meta}}) + (f_2 * \delta^{13}\text{C}_{\text{petrocarbon}}), \quad (13.4)$$

where $\delta^{13}\text{C}_{\text{meta}}$ is the $\delta^{13}\text{C}$ of metabolic carbon at the base of the food web for a given red snapper muscle sample, assumed here to be the mean of $\delta^{13}\text{C}_{\text{base}}$ estimated from the year prior to the DWH (-20.63‰); $\delta^{13}\text{C}_{\text{petrocarbon}}$ is $\delta^{13}\text{C}$ of petrocarbon [-57.4‰ for methane (Chanton et al. (2012) or -27.2‰ for petroleum (Graham et al. 2010)]; f_1 = fraction of $\delta^{13}\text{C}_{\text{base}}$ contributed by $\delta^{13}\text{C}_{\text{meta}}$; and f_2 = fraction of $\delta^{13}\text{C}_{\text{base}}$ contributed by petrocarbon, which equals $1 - f_1$. The model was solved for f_2 and then the percentage of $\delta^{13}\text{C}_{\text{base}}$ contributed by petrocarbon estimated as $100 * f_2$. With respect to muscle $\Delta^{14}\text{C}$, a similar mixing model was utilized:

$$\Delta^{14}\text{C}_{\text{muscle}} = (f_1 * \Delta^{14}\text{C}_{\text{meta}}) + (f_2 * \Delta^{14}\text{C}_{\text{petrocarbon}}), \quad (13.5)$$

where $\Delta^{14}\text{C}_{\text{muscle}}$ is the $\Delta^{14}\text{C}$ measured in a given red snapper muscle tissue sample; $\Delta^{14}\text{C}_{\text{meta}}$ is the metabolic $\Delta^{14}\text{C}$ assimilated in prey ingested by red snapper, assumed here to be the mean of pre-DWH red snapper muscle $\Delta^{14}\text{C}$ (50.7‰) given there is no trophic fractionation in $\Delta^{14}\text{C}$; $\Delta^{14}\text{C}_{\text{petrocarbon}}$ is the $\Delta^{14}\text{C}$ of petrocarbon, which is -1000‰ whether the source is petroleum or methane; f_1 = fraction of $\Delta^{14}\text{C}_{\text{muscle}}$ contributed by $\Delta^{14}\text{C}_{\text{meta}}$; and f_2 = fraction of $\Delta^{14}\text{C}_{\text{muscle}}$ contributed by petrocarbon, which equals $1 - f_1$. The model was solved for f_2 and then the percentage of $\Delta^{14}\text{C}_{\text{muscle}}$ contributed by petrocarbon estimated as $100 * f_2$.

The %petrocarbon in red snapper muscle tissue estimated with $\Delta^{14}\text{C}$ ranged from zero prior to the DWH to 2.2% ~ 2.5 years after the spill (Fig. 13.6a). One potential caveat is that utilizing mean pre-spill $\Delta^{14}\text{C}_{\text{muscle}}$ as one endpoint in the mixing model

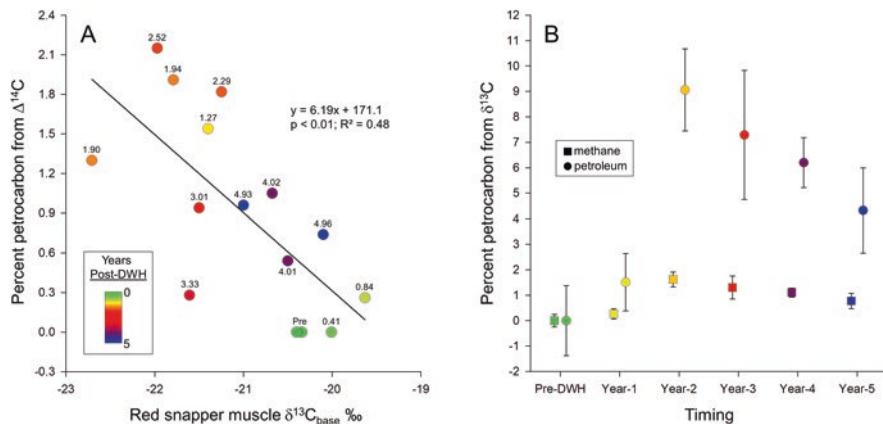


Fig. 13.6 The percentage ($\pm 95\%$ CIs) of adult red snapper muscle carbon with a petrocarbon origin estimated with mixing models for (a) $\Delta^{14}C$ ($n = 15$) and (b) $\delta^{13}C_{base}$ ($n = 400$) values measured in muscle tissue samples. Numbers next to symbols on plot indicate years post-DWH; P = pre-spill samples. The legend in panel A indicates collection timing for a given sample. In panel B, mixing models were computed with both methane (-57.4‰) and petroleum (-27.2‰) as potential $\delta^{13}C$; see text for details

would result in an underestimate of red snapper muscle %petrocarbon if petrocarbon contributed some percentage of organic carbon assimilated by red snapper prior to the DWH. However, the close correspondence between the pre-DWH mean $\delta^{13}C_{base}$ ($\pm 95\%$ CI) of -20.63‰ ($\pm 0.09\text{‰}$) to $\delta^{13}C$ of offshore GoM surface DOC (-20.7‰ ; Walker et al. 2017), which is a proxy for phytoplankton $\delta^{13}C$, suggests the assumption that zero petrocarbon was assimilated in red snapper muscle in the year prior to the DWH is valid.

Clearly, different estimates of %petrocarbon in red snapper muscle tissue computed with $\delta^{13}C$ result whether methane (-57.4‰) or petroleum (-27.2‰) is assumed to be the source of assimilated petrocarbon (Fig. 13.6b). Given the shorter distance in isotope space between $\delta^{13}C_{base}$ and the $\delta^{13}C$ of petroleum, the shifts observed in $\delta^{13}C_{base}$ in the years following the DWH yield higher estimates of %petrocarbon with oil-derived carbon rather than if methane was the source. The peak in %petrocarbon occurred in year-2 regardless of the petrocarbon endmember, with a mean ($\pm 95\%$ CI) of 1.62% ($\pm 0.29\%$) for methane versus 9.06% ($\pm 1.61\%$) for petroleum. The estimates produced with methane as an end-member most closely align with those produced with $\Delta^{14}C$; thus it is most likely that methane was the predominant source of petrocarbon assimilated in red snapper muscle tissue. Cherrier et al. (2013) similarly concluded that methane was the most likely contributor to petrocarbon in nGoM POC sampled in 2011 and 2012.

Overall, temporal shifts in red snapper muscle %petrocarbon were similar over the 6 study years whether $\delta^{13}C$ (assuming methane as the predominant petrocarbon source) or $\Delta^{14}C$ is examined. Both biomarkers produced peak estimates of $\sim 2\%$ petrocarbon contribution to the carbon assimilated in red snapper muscle tissue. Chanton et al. (2012) estimated nGoM plankton samples collected in 2010 and 2011

had a peak %petrocarbon of ~5%, while the greatest depletion in plankton $\delta^{13}\text{C}$ (-4‰) reported by Graham et al. (2010) in summer 2010 would yield a methane-based %petrocarbon estimate of ~10%. Among fish muscle samples, there was a 2- year lag between petrocarbon being assimilated by mesoplankton in summer 2010 and the peak in estimated red snapper muscle %petrocarbon, but the estimates for red snapper muscle suggest remarkable conservation of the petrocarbon signal through multiple trophic levels in the nGoM food web. This likely reflects not only the spatial extent of the spill and the volume of hydrocarbons released but also the duration of gas and oil availability to hydrocarbon-consuming bacteria (Joye et al. 2014). The time period of declining %petrocarbon in red snapper muscle, taking into account the ~6 month turnover time in the tissue (Nelson et al. 2011), is also consistent with the boom-bust cycle that was apparent in hydrocarbon-consuming bacteria populations in the years following the DWH (Dubinsky et al. 2013; Crespo-Medina et al. 2014; Joye et al. 2014).

13.3.2 *Potential Long-Term Biomarkers*

Muscle stable isotope or radioisotope signatures are ephemeral given tissue turnover; thus they are unable to provide a long-term biomarker of either trophic effects or the spatial extent of petroleum hydrocarbons in a marine ecosystem. Candidate structures in bony fishes that might be well suited for this purpose include otoliths or ear stones. Otoliths function in the acoustico-lateralis system of bony fishes where they occur in three pairs. The largest otoliths are the saggittae, which are routinely aged by counting annually formed opaque zones. Otoliths occur in a closed system, are principally composed (~95%) of aragonite (biogenic CaCO_3) in a protein matrix, and are metabolically inert once formed. The protein in otoliths has been extracted and its bulk and amino acid-specific $\delta^{13}\text{C}$ or $\delta^{15}\text{N}$ analyzed to estimate trophic position, habitat utilization, and food web structure (Huxam et al. 2007; McMahon et al. 2011; Lueders-Dumont et al. 2018). By mass, otoliths are ~10% C, with ~20–40% of that derived from metabolic carbon and the rest contributed by DIC (Høie et al. 2003; Tohse and Mugiya 2008). Given the time-keeping property of otoliths and the ability to discretely subsample growth zones with micromilling techniques (Barnett and Patterson 2010), otoliths may serve as ideal natural long-term biomarkers of trophic effects and petrocarbon assimilation following marine oil spills.

The potential for otoliths to serve as biomarkers of DWH-derived petrocarbon was tested with age-0 red snapper otoliths. Fish were sampled with trawls in October and November 2009–2013 (fish age ~120–150 days; Wells et al. 2008) on the nGoM shelf at water depths between 20 and 65 m. Samples were collected in two regions: the north central GoM in the region of the DWH spill (87° 30' W to 88° 45' W) and the southwest US GoM off Texas (94° 10' W to 95° 50' W). Fish were frozen in plastic bags and then stored in a freezer at -20 ° C. Later, fish ($n = 3$ per region per year) were thawed and their saggittal otoliths extracted with acid-leached glass

probes, rinsed of adhering tissue with double-deionized water, air dried under a class-10 clean hood, and stored dry in acid-leached polyethylene vials. The surface of dried otoliths was cleaned by immersion in 1% ultrapure HNO_3 for ~30 seconds and then repeatedly flooded with double-deionized water. Otoliths were again placed under a class-10 clean hood to air dry; then each was ground to a fine powder with an acid-leached mortar and pestle. Otolith powder (~10 mg) was transferred to glass vials that had been combusted at 500°C for 4 hours and then shipped to NOSAMS for $\delta^{13}\text{C}$ analysis with SIR-MS and $\Delta^{14}\text{C}$ analysis with AMS. Samples were processed for radiocarbon analysis as described above for muscle samples. Results are reported as $\Delta^{14}\text{C}$, which was corrected for natural isotopic fractionation via $\delta^{13}\text{C}$.

No red snapper samples were available for the north central GoM in fall 2011 due to poor red snapper recruitment in the eastern GoM the year following the DWH (SEDAR 2018). Otolith $\Delta^{14}\text{C}$ declined in both regions over the 5 study years, generally following the linear relationship reported by Barnett et al. (2018) for nGoM red snapper otolith $\Delta^{14}\text{C}$ versus year of formation (Fig. 13.7a). Observed otolith $\Delta^{14}\text{C}$ was subtracted from year-specific otolith $\Delta^{14}\text{C}$ values predicted from the Barnett et al. (2018) function to compute the residual value of individual samples (Fig. 13.7b). Ninety-five percent confidence intervals demonstrate mean $\Delta^{14}\text{C}$ residuals were not significantly different from zero (i.e., prediction) for both regions in all years, except for the north central GoM fish in 2010. In that year and region, age-0 red snapper had a mean ($\pm 95\%$ CI) otolith $\Delta^{14}\text{C}$ residual value of -6.13‰ ($\pm 2.64\text{‰}$). Age-0 red snapper otoliths have a mean %metabolic carbon of 34% (W. Patterson, unpublished data); thus the scaled total decline in metabolic $\Delta^{14}\text{C}$ would have been -18.0‰ . Given mixing model end-members of -1000‰ for

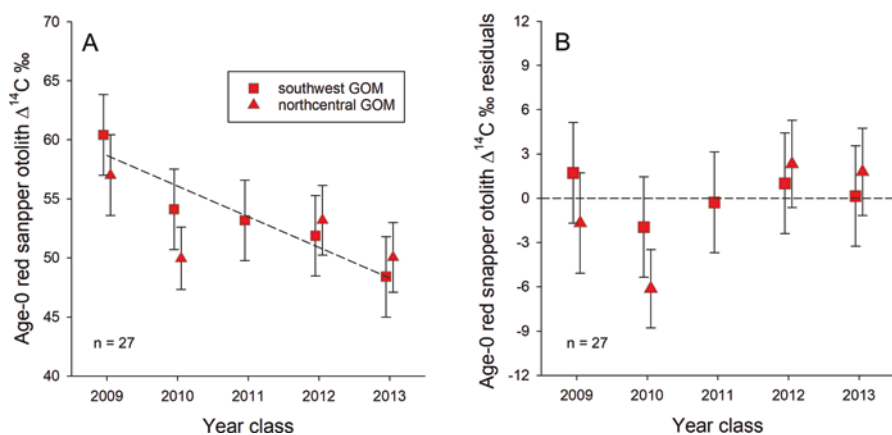


Fig. 13.7 (a) Plot of annual mean $\Delta^{14}\text{C}$ measured in whole age-0 red snapper otoliths ($n = 3$ per region per year) from the north central ($88^\circ 10'$ to $88^\circ 45'$ west) and southwest ($>94^\circ 10'$ west) US Gulf of Mexico from 2009 to 2013. Dashed line in panel A indicates the annual decline (-2.6‰ per year) in otolith core $\Delta^{14}\text{C}$ reported by Barnett et al. (2018) for northern Gulf of Mexico red snapper otoliths. (b) Residuals of annual mean age-0 otolith $\Delta^{14}\text{C}$ values relative to the predicted decline reported by Barnett et al. (2018) and plotted in panel A. Error bars in each panel are 95% confidence intervals

petrocarbon and approximately -40‰ for POM (Chanton et al. 2020), a scaled decline in $\Delta^{14}\text{C}$ of -18.0‰ would translate to petrocarbon constituting 1.73% of the metabolic carbon in fall 2010 north central GoM age-0 red snapper otoliths.

This estimated contribution of petrocarbon to age-0 red snapper otolith aragonite in fall 2010 is similar to that estimated for red snapper muscle 2–2.5 years after the DWH. This earlier incorporation of petrocarbon is likely due to age-0 red snapper feeding on lower trophic level prey, including plankton, that were already depleted in ^{14}C in summer and fall 2010 and also due to the fact that recently consumed metabolic carbon is precipitated on the rapidly growing otoliths of juvenile fishes (Høie et al. 2003; Tohse and Mugiya 2008). Therefore, there was no lag in petrocarbon incorporation in age-0 red snapper otoliths due to assimilation and tissue turnover processes like occurs with muscle or other tissues. It is unknown whether north central GoM age-0 red snapper had negative $\Delta^{14}\text{C}$ residual values in 2011 and if so whether they were similarly depleted or even to a greater extent than observed in fall 2010. One way to potentially examine that would be to analyze otolith cores of later-sampled subadult or adult north central GoM red snapper with 2010 birth years, but the older the fish, the greater the uncertainty they spent their early life in that region (Patterson 2007). What can be inferred from the otolith results is otolith $\Delta^{14}\text{C}$ appears to serve as an effective long-term biomarker of DWH petrocarbon. A larger sample, including some 2011 age-class fish from the north central GoM, would enable a more robust test of that premise, but results presented here are promising.

13.4 Summary and Implications for Future Marine Oil Spills

The clear petrocarbon signature in mesopredator reef fish muscle sampled from a broad ($\sim 7500\text{ km}^2$) region of the north central GoM shelf in the years following the DWH provides strong support that $\Delta^{14}\text{C}$ and $\delta^{13}\text{C}$ can be utilized as natural biomarkers of the spatial extent of food web effects of marine oil spills. The advantages of utilizing $\Delta^{14}\text{C}$ as biomarker in this context are it providing higher resolution due to larger differences between tissue and petroleum endmember values, as well as having a common end-member value (-1000‰) regardless of the petrocarbon source. A key disadvantage is the cost of analysis ($\sim \$325\text{US}$ for $\Delta^{14}\text{C}$ versus $\sim \$15\text{US}$ for $\delta^{13}\text{C}$ in 2018), given both stable carbon and radiocarbon isotopes can provide valuable information about the extent, timing, and duration of petrocarbon assimilation. While assimilation and trophic transfer of petrocarbon in the nGoM food web are not evidence, per se, of food web effects, they do indicate in the case of the DWH the persistent presence of petroleum hydrocarbons in the ecosystem in the years following the spill.

Trophic effects inferred from red snapper muscle $\delta^{15}\text{N}$ and $\delta^{34}\text{S}$, and from $\delta^{15}\text{N}$ alone in muscle samples from a suite of other reef fishes, do clearly demonstrate the overlap of food web effects and petrocarbon assimilation in the food web. Muscle tissue signatures are ephemeral, given tissue turnover, and thus did not provide a

long-term biomarker of either trophic effects or the spatial extent of petroleum hydrocarbons in the system. However, chemical signatures in otoliths likely do provide long-term trophic and petrocarbon biomarkers that could be utilized to examine temporal and spatial dynamics of DWH food web effects or those caused by other large-scale marine oil spills. Regardless of the question, or the tissue or structure utilized as a biogeochemical marker to examine it, results here clearly indicate the value of baseline data, without which no reference to assess potential post-spill shifts would be possible.

Acknowledgments Reef fish samples described herein were collected during cooperative research with for-hire recreational fishermen in the nGoM. We thank Captains Johnny Greene, Gary Jarvis, Sean Kelley, and Seth Wilson for their contributions, as well as numerous volunteers who helped procure samples. We thank Miaya Glabach and Samantha Bosman for processing samples for $\delta^{13}\text{C}$ and $\Delta^{14}\text{C}$ analysis and Sue Handwork, Kathy Elder, and Ann McNichol at WHOI-NOSAMS and Alexander Cherkinsky at UGA-CIAS for $\delta^{13}\text{C}$ and $\Delta^{14}\text{C}$ analysis.

Funding Information In addition to the Gulf of Mexico Research Initiative (GoMRI) funding through the C-IMAGE consortium, this research was also made possible by grants from the Florida Institute of Oceanography, a grant from the Florida Department of Environmental Protection, and a grant from the Florida Fish and Wildlife Research Institute. All data presented herein are publicly available through the Gulf of Mexico Research Initiative Information and Data Cooperative (GRIIDC): <https://data.gulfresearchinitiative.org/data/Y1.x049.000:0007> and <https://data.gulfresearchinitiative.org/data/R4.x267.180:0021>.

References

- Barnett BK, Patterson WF III (2010) The effect of coring and pulverizing juvenile red snapper, *Lutjanus campechanus*, otoliths on their chemical signatures. *Environ Biol Fish* 89(3–4):463–417. <https://doi.org/10.1007/s10641-010-9697-7>
- Barnett BK, Thorton LR, Allman RJ, Chanton JP, Patterson WF III (2018) Linear decline in red snapper (*Lutjanus campechanus*) otolith $\Delta^{14}\text{C}$ extends the utility of the bomb radiocarbon chronometer for fish age validation in the Northern Gulf of Mexico. *ICES J Mar Sci* 75(5):1664–1771. <https://doi.org/10.1093/icesjms/fsy043>
- Beyer J, Trannum HC, Bakke T, Hodson PV, Collier TK (2016) Environmental effects of the Deepwater Horizon oil spill: a review. *Mar Pollut Bull* 110:28–51. <https://doi.org/10.1016/j.marpolbul.2016.06.027>
- Bosman SH, Chanton J, Rogers KL (2017) Using stable and radiocarbon analyses as a forensic tool to find evidence of oil in the particulates of the water column and on the seafloor following the 2010 Gulf of Mexico Oil Spill. In: Stout S, Wang Z (eds) *Case studies in Oil Spill environmental forensics*. Academic Press. <https://doi.org/10.1016/B978-0-12-804434-6.00029-X>
- Chanton JP, Cherrier J, Wilson RM, Sarkodee-Adoo J, Bosman S, Mickel A, Graham WM (2012) Radiocarbon evidence that carbon from the Deepwater Horizon spill entered the planktonic food web of the Gulf of Mexico. *Environ Res Lett* 7:045303. <https://doi.org/10.1088/1748-9326/7/4/045303>
- Chanton JP, Jaggi A, Radović JR, Rosenheim BE, Walker BD, Larter SR, Rogers K, Bosman S, Oldenburg TBP (2020) Mapping isotopic and dissolved organic matter baselines in waters and sediments of Gulf of Mexico (Chap. 10). In: Murawski SA, Ainsworth C, Gilbert S, Hollander D, Paris CB, Schlüter M, Wetzel D (eds) *Scenarios and responses to future Deep Oil Spills – fighting the next war*. Springer, Cham

- Chasar LC, Chanton JP, Koenig CC, Coleman FC (2005) Evaluating the effect of environmental disturbance on the trophic structure of Florida Bay, USA: multiple stable isotope analyses of contemporary and historical specimens. *Limnol Oceanogr* 50(4):1059–1072. <https://doi.org/10.4319/lo.2005.50.4.1059>
- Cherrier J, Sarkodee-Adoo J, Guilderson TP, Chanton JP (2013) Fossil carbon in particulate organic matter in the Gulf of Mexico following the Deepwater Horizon event. *Environ Sci Tech Lett* 2014(1):108–112. <https://doi.org/10.1021/ez400149c>
- Crespo-Medina M, Meile CD, Hunter KS, Diercks AR, Asper VL, Orphan VJ, Tavormina PL, Nigro LM, Battles JJ, Chanton JP, Shiller AM, Joung DJ, Amon RMC, Bracco A, Montoya JP, Villareal TA, Wood AM, Joye SB (2014) The rise and fall of methanotrophy following a Deepwater oil-well blowout. *Nat Geosci* 7:423–427. <https://doi.org/10.1038/NNGEO2156>
- Dubinsky EA, Conrad ME, Chakraborty R, Bill M, Borglin SE, Hollibaugh JT, Mason OU, Piceno YM, Reid FC, Stringfellow WT, Tom LM, Hazen TC, Andersen GL (2013) Succession of hydrocarbon-degrading bacteria in the aftermath of the Deepwater Horizon Oil Spill in the Gulf of Mexico. *Environ Sci Technol* 47:10860–10867. <https://doi.org/10.1021/es401676y>
- Fodrie FJ, Able KW, Galvez F, Heck KL Jr, Jensen OP, Lopez-Duarte PC, Martin CW, Turner RE, Whitehead A (2014) Integrating organismal and population responses of estuarine fishes in Macondo spill research. *Bioscience* 64:778–788. <https://doi.org/10.1093/biosci/biu123>
- Fry B (2006) Stable isotope ecology. Springer-Verlag, New York
- Fry B, Chumchal MC (2011) Sulfur stable isotope indicators of residency in estuarine fish. *Limnol Oceanogr* 56(5):1563–1576. <https://doi.org/10.4319/lo.2011.56.5.1563>
- Gin KYH, Huda MK, Lim WK, Tkalic P (2001) An oil-spill food chain interaction model for coastal seas. *Mar Pollut Bull* 42(7):590–597. [https://doi.org/10.1016/S0025-326X\(00\)00205-8](https://doi.org/10.1016/S0025-326X(00)00205-8)
- Goldman SF, Glasgow DM, Falk MM (2016) Feeding habits of 2 reef-associated fishes, red porgy (*Pagrus pagrus*) and gray triggerfish (*Balistes capricus*), off the southeastern United States. *US Fish Bull* 114(3):317–329. <https://doi.org/10.7755/FB.114.3.5>
- Graham WM, Condon RH, Carmichael RH, D'Ambra I, Patterson HK, Linn LJ, Hernandez FJ Jr (2010) Oil carbon entered the coastal planktonic food web during the Deepwater Horizon oil spill. *Environ Res Lett* 5:045301. <https://doi.org/10.1088/1748-9326/5/4/045301>
- Grimes CB (1979) Diet and feeding ecology of vermilion snapper, *Rhomboplites aurorubens* (Cuvier) from North Carolina and South Carolina waters. *Bull Mar Sci* 29(1):53–61
- Grottoli AG, Eakin CM (2007) A review of modern coral $\delta^{18}\text{O}$ and $\Delta^{14}\text{C}$ proxy records. *Earth Sci Rev* 81:67–91. <https://doi.org/10.1016/j.earscirev.2006.10.001>
- Høie H, Folkvord A, Otterlei E (2003) Effect of somatic and otolith growth rate on stable isotopic composition of early juvenile cod (*Gadus morhua* L) otoliths. *J Exp Mar Biol Ecol* 289:41–58. [https://doi.org/10.1016/S0022-0981\(03\)00034-0](https://doi.org/10.1016/S0022-0981(03)00034-0)
- Holmer M, Marba N, Diaz-Almela E, Duarte CM, Tsapakis M, Danovaro R (2007) Sedimentation of organic matter from fish farms in oligotrophic Mediterranean assessed through bulk and stable isotope ($\delta^{13}\text{C}$ and $\delta^{15}\text{N}$) analyses. *Aquaculture* 262:268–280. <https://doi.org/10.1016/j.aquaculture.2006.09.033>
- Huxam M, Kimani E, Newton J, Augley J (2007) Stable isotope records from otoliths as tracers of fish migration in a mangrove system. *J Fish Biol* 70:1554–1567. <https://doi.org/10.1111/j.1095-8649.2007.01443.x>
- Jennings S, Greenstreet SPR, Hill L, Piet GJ, Pinnegar JK, Warr KJ (2002) Long-term trends in the trophic structure of the North Sea fish community: evidence from stable-isotope analysis, size-spectra and community metrics. *Mar Biol* 141:1085–1097. <https://doi.org/10.1007/s00227-002-0905-7>
- Joye SB, Teske AP, Kostka JE (2014) Microbial dynamics following the Macondo oil well blowout across Gulf of Mexico environments. *Bioscience* 64:766. <https://doi.org/10.1093/biosci/biu121>
- Kurz RC (1995) Predator-prey interactions between gray triggerfish (*Balistes capricus* Gmelin) and a guild of sand dollars around artificial reefs in the northeastern Gulf of Mexico. *Bull Mar Sci* 56(1):150–160
- Leboulanger C, Descolas-Gros C, Fontugne MR, Bentaleb HJ (1995) Interspecific variability and environmental influence on particulate organic carbon $\delta^{13}\text{C}$ in cultured marine phytoplankton. *J Plankton Res* 17(11):2079–2091

- Lueders-Dumont JA, Wang XT, Jensen OP, Sigman DM, Ward BB (2018) Nitrogen isotopic analysis of carbonate-bound organic matter in modern and fossil fish otoliths. *Geochim Cosmochim Acta* 224:200–222. <https://doi.org/10.1016/j.gca.2018.01.001>
- Manooch CS (1977) Foods of the red porgy, *Pagrus pagrus* Linnaeus (Pisces: Sparidae), from North Carolina and South Carolina. *Bull Mar Sci* 27(4):776–787
- McCann MJ, Able KW, Christian RR, Fodrie FJ, Jensen OP, Johnson JJ, Lopez-Duarte PC, Martin CW, Olin JA, Polito MJ, Roberts BJ, Ziegler SL (2017) Key taxa in food web responses to stressors: the Deepwater Horizon oil spill. *Front Ecol Environ* 15(3):142–149. <https://doi.org/10.1002/fee.1474>
- McCawley JR, Cowan JH Jr, Shipp RL (2003) Red snapper (*Lutjanus campechanus*) diet in the north-central Gulf of Mexico on Alabama artificial reefs. *Proc Gulf Caribb Fish Inst* 54:372–385
- McCutchan JH Jr, Lewis WM Jr, Kendall C, McGrath CC (2003) Variation in trophic shift for stable isotope ratios of carbon, nitrogen, and sulfur. *Oikos* 102:378–390. <https://doi.org/10.1034/j.1600-0706.2003.12098.x>
- McMahon KW, Fogel ML, Johnson BJ, Houghton LA, Thorrold SR (2011) A new method to reconstruct fish diet and movement patterns from $\delta^{13}\text{C}$ values in otolith amino acids. *Can J Fish Aquat Sci* 68:1330–1340. <https://doi.org/10.1139/F2011-070>
- Moncrieff CA, Sullivan MJ (2001) Trophic importance of epiphytic algae in subtropical seagrass beds: evidence from multiple stable isotope analyses. *Mar Ecol Prog Ser* 215:93–106
- Nelson J, Chanton J, Coleman F, Koenig C (2011) Patterns of stable carbon isotope turnover in gag, *Mycteroperca microlepis*, an economically important marine piscivore determined with a non-lethal surgical biopsy procedure. *Environ Biol Fish* 90(3):243–252. <https://doi.org/10.1007/s10641-010-9736-4>
- Norberg MA (2015) Effects of the Deepwater Horizon Oil Spill and habitat type on the ecology of tomatate, *Haemulon aurolineatum*, in the northern Gulf of Mexico. University of South Alabama, Mobile, 81 pp
- Olin JA, Bergeon Burns CM, Woltmann S, Taylor SS, Stouffer PC, Bam W, Hooper-Bui L, Turner RE (2018) Seaside Sparrows reveal contrasting food web responses to large-scale stressors in coastal Louisiana saltmarshes. *Ecosphere* 8(7):e01878. <https://doi.org/10.1002/ecs2.1878>
- Patterson WF III (2007) A review of Gulf of Mexico red snapper movement studies: implications for population structure. *Am Fish Soc Symp* 60:221–236
- Peterson CH, Rice SD, Short JW, Esler D, Bodkin JL, Ballachey BE, Irons DB (2003) Long-term ecosystem response to the Exxon Valdez Oil Spill. *Science* 302:2082–2086. <https://doi.org/10.1126/science.1084282>
- Post DM, Layman CA, Arrington DA, Takimoto G, Quattrochi J, Montana CG (2007) Getting to the fat of the matter: models, methods and assumptions for dealing with lipids in stable isotope analyses. *Oecologia* 152:179–189. <https://doi.org/10.1007/s00442-006-0630-x>
- Radabaugh KR, Hollander DJ, Peebles EB (2013) Seasonal $\delta^{13}\text{C}$ and $\delta^{15}\text{N}$ isoscapes of fish populations along a continental shelf trophic gradient. *Cont Shelf Res* 68:112–122. <https://doi.org/10.1016/j.csr.2013.08.010>
- Rooker JR, Turner JP, Holt SA (2006) Trophic ecology of *Sargassum*-associated fishes in the Gulf of Mexico determined from stable isotopes and fatty acids. *Mar Ecol Prog Ser* 313:249–259
- Sedberry GR (1985) Food and feeding of the tomatate, *Haemulon aurolineatum* (Pisces, Haemulidae), in the South Atlantic Bight. *US Fish Bull* 83(3):461–466
- Southeast Fishery Assessment and Review (SEDAR) (2018) SEDAR 52 stock assessment report Gulf of Mexico Red Snapper. South Atlantic Fishery Management Council, Charleston, South Carolina. 435 pp. <http://sedarweb.org/sedar-52>, Accessed 1 Oct 2018
- Stuiver M, Pollach HA (1977) Discussions of reporting ^{14}C data. *Radiocarbon* 19:355–363
- Sweeting CJ, Barry J, Barnes C, Polunin NVC, Jennings S (2007) Effects of body size and environment on diet-tissue $\delta^{15}\text{N}$ fractionation in fishes. *J Exp Mar Biol Ecol* 340:1–10. <https://doi.org/10.1016/j.jembe.2006.07.023>
- Tarnecki JH, Patterson WF III (2015) Changes in red snapper, *Lutjanus campechanus*, diet and trophic ecology in the northern Gulf of Mexico following the Deepwater Horizon Oil Spill. *Marine and Coastal Fisheries* 7:135–147. <https://doi.org/10.1080/19425120.2015.1020402>

- Tarnecki JH, Wallace A, Simons J, Ainsworth CH (2016) Progression of a Gulf of Mexico food web supporting Atlantis ecosystem model development. *Fish Res* 179:237–250. <https://doi.org/10.1016/j.fishres.2016.02.023>
- Tohse H, Mugiya Y (2008) Sources of otolith carbonate: experimental determination of carbon incorporation rates from water and metabolic CO₂, and their diel variations. *Aquat Biol* 1:259–268. <https://doi.org/10.3354/ab00029>
- Vanderklift MA, Ponsard S (2003) Sources of variation in consumer-diet δ¹⁵N enrichment: a meta-analysis. *Oecologia* 136:169–182. <https://doi.org/10.1007/s00442-003-1270-z>
- Vose FE, Nelson WG (1994) Gray triggerfish (*Balistes capriscus* Gmelin) feeding from artificial and natural substrate in shallow Atlantic waters of Florida. *Bull Mar Sci* 55(2–3):1316–1323
- Walker BD, Druffel ERM, Kolasinski J, Roberts BJ, Xu X, Rosenheim BE (2017) Stable and radiocarbon isotopic composition of dissolved organic matter in the Gulf of Mexico. *Geophys Res Lett* 44:8424–8434. <https://doi.org/10.1002/2017GL074155>
- Wells RJD, Cowan JH Jr, Patterson WF III, Walters CJ (2008) Effect of trawling on juvenile red snapper (*Lutjanus campechanus*) habitat selection and life history parameters. *Can J Fish Aquat Sci* 65(11):2399–2411. <https://doi.org/10.1139/F08-145>
- Wilson RM, Cherrier J, Sarkodee-Adoo, Bosman S, Mickle A, Chanton JP (2016) Tracing the intrusion of fossil carbon into coastal Louisiana macrofauna using natural ¹⁴C and ¹³C abundances. *Deep Sea Res II* 129:89–95. <https://doi.org/10.1016/j.dsr2.2015.05.014>